Since January 2020 Elsevier has created a COVID-19 resource centre with free information in English and Mandarin on the novel coronavirus COVID-19. The COVID-19 resource centre is hosted on Elsevier Connect, the company's public news and information website.

Virology 436 (2013) 24–32

Contents lists available at SciVerse ScienceDirect

Virology

journal homepage: www.elsevier.com/locate/yviro

Substrate specificity of Tulane virus protease

Chao Wei [a], Jarek Meller [c], Xi Jiang [a,b,*]

[a] Division of Infectious Diseases, Cincinnati Children's Hospital Medical Center, Cincinnati, OH, USA
[b] Department of Pediatrics, University of Cincinnati College of Medicine, Cincinnati, OH, USA
[c] Department of Environmental Health, University of Cincinnati College of Medicine, Cincinnati, OH, USA

ARTICLE INFO

Article history:
Received 10 September 2012
Returned to author for revisions
26 September 2012
Accepted 5 October 2012
Available online 8 November 2012

Keywords:
Tulane virus
Calicivirus
Human norovirus
Viral protease
Polyprotein cleavage

ABSTRACT

Tulane virus (TV) is a cultivable calicivirus isolated from rhesus monkeys. In this study, we characterized the substrate specificity of TV protease *in trans* using recombinant proteases and TV polyprotein fragments containing the predicted proteolytic cleavage sites. Cleavage products have been obtained from 4 of the 5 fragments containing ^{573}Q–S^{574} between the helicase and 3A-like protein, ^{712}E–A^{713} between the 3A-like protein and Vpg, ^{802}E–G^{803} between Vpg and the protease, and ^{976}E–G^{977} between the protease and RdRp. We also characterized the enzymatic activities of the recombinant proteases of TV and Norwalk virus using synthetic fluorogenic peptide substrates. Under optimal conditions for enzymatic assays, partial cross-reactivities on reciprocal substrates were observed between TV and Norwalk virus proteases. The apparently shared substrate specificities between TV and Norwalk virus proteases suggested that the cultivable TV could be used as a model for in vivo evaluation of lead candidates of protease inhibitors for human norovirus.

Introduction

Caliciviruses (CVs) are small, non-enveloped, positive-stranded RNA viruses. Members of the CV family can cause a wide variety of diseases in humans and animals, including respiratory infections, vesicular lesions, gastroenteritis, and hemorrhagic diseases. Norovirus (NoV) belongs to one of the five genera of CVs which mainly infects humans and causes acute gastroenteritis in all age groups (Glass et al., 2009). Currently, there are no effective treatments or vaccines available against NoVs. The lack of a cell culture system or animal model for NoVs has been a major hurdle for studies of NoV replication and pathogenesis.

Tulane virus (TV) is a CV isolated recently from stools of rhesus monkeys. Like most other CVs, the TV genome encodes three open reading frames (ORFs). ORF1 encodes a non-structural polyprotein, whereas ORF2 and ORF3 encode a major and a minor structural protein, respectively (Farkas et al., 2008; Glass et al., 2000; Jiang et al., 1993). TV has a similar genome organization as other CVs, and has been proposed to comprise a new genus, named recovirus (Farkas et al., 2008). Evolutionarily, TV is more closely related to NoVs than to any other genera of *Caliciviridae* (Farkas et al., 2008). At a total of 6714 nucleotides (nt) in length, TV represents the smallest genome in the CV family. TV has been successfully cultivated in the rhesus monkey kidney cell line LLC-MK2 and causes cytopathic effect (CPE) upon infection of these cells. A reverse genetics system of TV has been established, which makes TV an ideal surrogate for NoV studies (Wei et al., 2008).

The CV non-structural polyprotein is known to be processed into six functional proteins by the viral 3C like protease (Blakeney et al., 2003), which plays an essential role in maturation of functional proteins and virus replication, as well as pathogenesis. The crystallographic structures of several NoV proteases have been elucidated (Hussey et al., 2010; Nakamura et al., 2005; Zeitler et al., 2006). These data suggest that NoV proteases form dimers (Nakamura et al., 2005; Zeitler et al., 2006) and display a trypsin or chymotrypsin-like serine protease fold, involving a nucleophilic cysteine thiol (at amino acid residue 139) in the catalytic triad (Zeitler et al., 2006). Two other critical residues in the catalytic site, completing the catalytic triad, are a histidine at position 30 and a glutamic acid at position 54 (Zeitler et al., 2006). Alignments of amino acid sequences for TV, NoV, and other CV proteases revealed that the critical residues in the catalytic triad are well conserved.

The proteases of the CV family cleave substrates between Glu or Gln in the P1 position and various amino acid residues, such as Ala and Gly in the P1′ position (Belliot et al., 2003; Blakeney et al., 2003; Joubert et al., 2000; Liu et al., 1999; Oka et al., 2005; Robel et al., 2008; Sosnovtsev et al., 2006, 2002; Wirblich et al., 1995). Amino acid residues adjacent to P1–P1′ positions may also affect substrate specificities and cleavage efficiencies (Oka et al., 2009; Someya and Takeda, 2009). Sequence alignments of the

* Corresponding author at: University of Cincinnati College of Medicine, Division of Infectious Diseases, Cincinnati Children's Hospital Medical Center, 3333 Burnet Ave, Cincinnati, Ohio 45229-3039, USA. Fax: +513 636 7655.
E-mail address: jason.jiang@cchmc.org (X. Jiang).

0042-6822/$ - see front matter © 2012 Elsevier Inc. All rights reserved.
http://dx.doi.org/10.1016/j.virol.2012.10.010

nonstructural polyproteins of TV and other CVs with known polyprotein cleavage maps revealed the presence of putative cleavage sites in the TV polyprotein (Farkas et al., 2008). However, the precise proteolytic cleavages of TV polyprotein have not been analyzed to date.

Here we report an investigation into the proteolytic processing of the TV nonstructural polyprotein in vitro using *E. coli*-expressed protease and polyprotein fragments. N-terminal sequencing of four cleaved products indicated that these cleavages occur precisely at the predicted sites, which suggests conservation of the substrate specificities between the TV protease and other CV proteases. We also characterized the enzymatic activities of the recombinant TV protease and NoV protease using recombinant polyprotein fragments and fluorescence resonance energy transfer (FRET) assays. Our results demonstrated that the fluorescence-based assay is sensitive and reliable for the evaluation of CV protease activities, and that the cultivable TV could be used as a model for in vivo validation of lead protease inhibitor candidates.

Results

Expression and purification of recombinant proteases. To obtain an adequate amount of proteases for enzymatic characterization, we expressed the TV and a NoV (the Norwalk virus) proteases as the GST or histidine (His) tagged fusion proteins, as suggested by Zeitler et al. (Zeitler et al., 2006). Both the GST- and His-tag proteins were soluble and readily purified using non-denaturing affinity purification methods. The purified enzymes appeared homogeneous by the SDS-polyacrylamide gel electrophoresis (PAGE) and FPLC analyses (Fig. 1). Purified proteases with the His-tag or after removal of the GST tag appeared as monomers in solution for both TV and Norwalk virus proteases by comparison with the chymotrypsinogen A standard (molecular weight of 20.4 kDa) in the FPLC analysis (data not shown).

Proteolytic cleavage between the helicase and 3A-like protein. To facilitate the proteolitic analysis of TV polyprotein, recombinant protein fragments containing different regions of the polyprotein were produced. To analyze the cleavage site between the helicase and 3A-like protein, the coding region for amino acid residues 495 to 795 was expressed as a MBP fusion protein (79.7 kDa; Fig. 2A, F2). Proteolytic cleavage of this protein by the TV protease yielded four major bands at approximately 54 kDa, 45 kDa, 30 kDa, and 16 kDa respectively. Two of which were readily detected by a TV 3A-like protein specific antibody in a Western blot analysis: a ~30 kDa fragment was likely to contain the 3A-like protein-VpG, while the 16 kDa fragment was the 3A-like protein (Fig. 2B, lane 5). The identity of the 3A-like protein-VpG fragment was further confirmed by N-terminal sequencing. The resulting amino acid sequence "SDEYP" was identical to the expected N-terminus of the functional 3A-like protein.

Proteolytic cleavage between the 3A-like protein and Vpg. Due to a small size upon the cleavage by protease, the Vpg protein (10.8 kDa) is difficult to isolate from a PAGE gel for N-terminal sequencing analysis. Hence, a double fusion protein containing a protein fragment from amino acid residues 632 to 779 with the predicted cleavage site flanked by the MBP and GST at the N- and C-termini, respectively (Fig. 2A, F3) was expressed. Proteolytic cleavage of this protein by the TV protease yielded a 42 kDa band that was expected to be the MBP, a 32 kDa protein of the VpG-GST fusion protein, and an unknown band of ~19 kDa (Fig. 2C). The N-terminal sequencing of the 32 kDa protein revealed a sequence "AKGKT" that was the expected N-terminal sequences of the VpG-GST fusion protein.

Proteolytic cleavage between Vpg and the protease. The TV polyprotein fragment containing the cleavage site between Vpg and protease was fused to MBP at the N-terminus (Fig. 2A, F4). To prevent potential auto-cleavage of the protease, we replaced residue C134 with an A134 at the catalytic site of the protease. Since the cleaved protease fragment from F4 would be the same size as the active protease *in trans*, we fused GST to the C-terminus of the protease. Upon cleavage, two cleavage products, the 52.2 kDa MBP-VpG C-terminus and the 44.7 kDa protease-GST, were produced. N-terminal sequencing analysis of the 44.7 kDa fragment resulted in a perfect match to all of three amino acid residues detected with the predicted N-terminal sequence of TV protease (Fig. 3A).

Proteolytic cleavage between the protease and RdRp. The TV polyprotein fragment containing the cleavage site between the protease and RdRp (Fig. 2A, F5) was fused to GST at the N-terminus. The cleavage of the 96.9 kDa F5 fragment was expected to generate at least five smaller fragments: the 52.9 kDa RdRp, the 18 kDa protease, the 70.9 kDa protease-RdRp, the 44 kDa GST-protease, and the 26 kDa GST. The N-terminus sequencing of the 52.9 kDa fragment (RdRp) showed a perfect match of the first five amino acid residues GKTTY (Fig. 3B) with that of the predicted RdRp.

Proteolytic cleavage between the NTP and helicase proteins. We have also attempted to express a protein fragment containing the protease cleavage site between the N-terminal protein and helicase protein using similar fusion expression strategies (Fig. 2A, F1). Unfortunately, despite tremendous efforts, we were

Table 1
Primers used for the amplification of NoV protease, TV protease, and TV polyprotein fragment cDNAs.

Primers	Sequence	Restriction enzyme site	Orientation	Amplifications
P1405b	CGCGGATCCGCTCCCCCGACACTATGGAGCCGAG	BamHI	Forward	NoV protease
P1406	ATGGTCGACTCATTCTAGTGCGGTTTCGCC	SalI	Reverse	
P1069c	CGCGGATCCGTGTGTTCTTTTGTCTTC	BamHI	Forward	TV protease
P1071b	ATAGTCGACTCACCCTTCAAGGTTGAATCTAGAAG	SalI	Reverse	
p1282b	ACTGGTACCTCAGATGAATATCCAGAGC	KpnI	forward	TV 3Al
p1283b	ATGGTCGACTCACTCAAACACGCTAAGTGC	SalI	Reverse	
P1095	AATGGATCCATGGATACGTCCATAGATTC	BamHI	Forward	Polyprotein F1
P1077	ATAGTCGACTCAGGAGCATCCCAACTGGAG	SalI	Reverse	
P1403	TGGAATTCACCACAAACTTGGAGGAC	EcoRI	Forward	Polyprotein F2
P1404	ATGGTCGACTCACTCGTCGTAATAATCATCACT	SalI	Reverse	
P1890	TGAGGATCCCTCGATGGATACCTCACTG	BamHI	Forward	Polyprotein F3
P1891	ACTGTCGACCACCACTCATCATCTTC	SalI	Reverse	
P1069	CGCGGATCCCCCAGTGATGATTATTACGAC	BamHI	Forward	Polyprotein F4
P1071c	GCAGTCGACAGGTTGAATCTAGAAGGTATC	SalI	Reverse	
P1069	CGCGGATCCCCCAGTGATGATTATTACGAC	BamHI	Forward	Polyprotein F5
P1079	ATAGTCGACTCACAAGAATCCAGAACAACC	SalI	Reverse	

unable to express any protein fragment containing the C-terminal portion of the N-terminal protein in either GST- or MBP- fusion, or his-tagged forms.

Characterization of the enzymatic activities of the TV and Norwalk virus proteases with fluorogenic peptide substrates. As demonstrated in the above polyprotein cleavage analysis, *E.coli*-expressed proteases remain active upon purification, which makes possible to develop an in vitro antiviral screening system. To this end, we evaluated the Norwalk virus protease activities and the TV protease activities using synthetic fluorogenic peptide substrates NVS1 and TVS2 (Fig. 4A). In the presence of 2 nM NVS1, as shown in Fig. 4(B), a dose response of enzyme activities was observed in the reactions containing less than 5 μM of protease, which was followed by a plateau at protease concentrations between 5 and 20 uM. A similar fluorescence emission profile was also observed when the fluorogenic peptide substrate TVS2 was hydrolyzed by TV protease (Fig. 4C). These results indicate that Hylite Fluor 488/QXL520-labled peptide substrates are ideal for measuring recombinant Norwalk virus and TV protease activities.

To determine the optimal reaction conditions for Norwalk virus protease activity assay, we also performed the assays at various pH, salt, glycerol and DMSO concentrations. At a constant ionic strength (50 mM NaCl), the optimal pH for proteolytic cleavage of Norwalk virus protease was found to be pH 8.5 (Fig. 5A), similar to that reported previously for NoV (Someya et al., 2005) and for the NS3 protease of Dengue-2 virus (Leung et al., 2001). The Norwalk virus protease activities decreased significantly as the NaCl concentration rose (from 50 mM to 300 mM, Fig. 5B). In contrast, glycerol in the reaction solution seemed to promote protease activities (Fig. 5C). Based on these observations, we used this buffer condition (50 mM Tris, pH 8.5, 20% glycerol, and 1 mM DTT) for all of our protease activity assays. DMSO at concentrations less than 10% did not affect either the Norwalk virus or TV protease activities.

The TV and Norwalk virus proteases can partially cleavage heterologous substrates. Although the TV and NoV proteases share less than 27% amino acid sequence identity, the catalytic triads are highly conserved (Fig. 6A), indicating that the TV and NoV proteases may be able to process each other's polyprotein substrates. To test this hypothesis, we incubated the TV and Norwalk virus proteases with each other's substrates, and found that both enzymes were able to cleave each other's substrates, although the relative enzymatic activities were around 30–40%, compared with that on their native substrates (Fig. 6(B) and (C)).

Inhibition of the Norwalk virus protease activities. Since CV proteases are cysteine proteases that display a trypsin or chymotrypsin-like serine protease specificity, we tested whether common cysteine and serine protease inhibitors could inhibit the enzymatic activities of the Norwalk virus protease (Fig. 7A). Among five inhibitors tested: E64, leupeptin, phenylmethyl sulfonyl fluroride (PMSF), 1-Chloro-3-tosylamido-4-phenyl-2-butanone (TPCK), and 1-Chloro-3-tosylamido-7-amino-2-heptanone HCl (TLCK), four – leupeptin, TPCK, TLCK, and PMSF – revealed suppressive effects on NoV protease activities, with an IC_{50} of 18.8 μM for TPCK (Fig. 7B) and 175.1 μM for TLCK (Fig. 7C). These results are consistent with a report by Blakeney et al. (Blakeney et al., 2003).

Discussion

Many RNA viruses encode their functional proteins in a single open reading frame, where the proteins are translated as a polyprotein prior to being processed by a viral protease into individual functional proteins. Thus, the viral protease plays an essential role in virus replication and pathogenesis. Like that of picornaviruses, the CV proteases utilize a cysteine residue at its catalytic site as a nucleophile (Zeitler et al., 2006). Based on sequence alignments of several CV nonstructural proteins, we previously predicted the

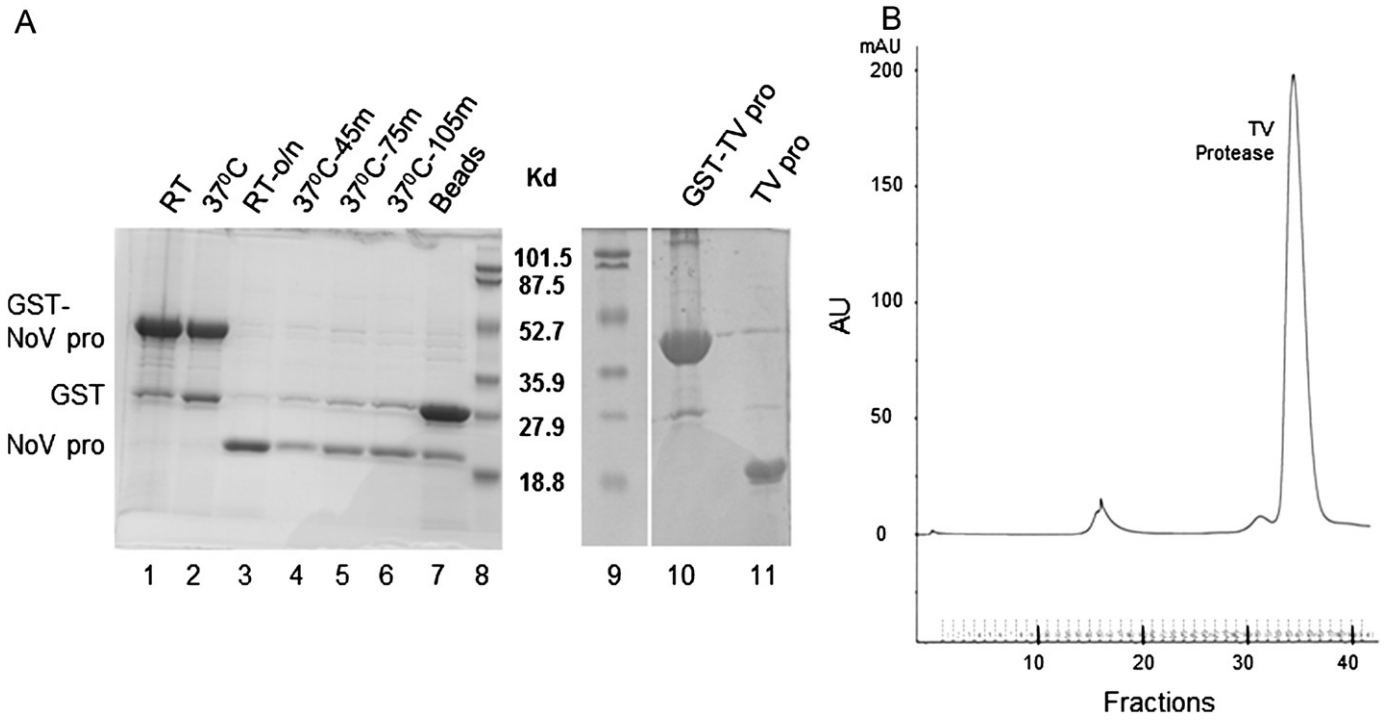

Fig. 1. Purification of NoV and TV proteases. (A) Lane 1&2, purified GST-NoV protease fusion protein expressed at room temperature and at 37 °C; Lane 3-6, NoV protease released by thrombin digestion under various conditions. Lane 7, GST protein bound on the beads. Lane 8, and 9, protein markers. Lane 10, purified GST-TV protease fusion protein. Lane 11, TV protease released by thrombin digestion. (B) FPLC profile of purified TV protease.

location of the TV protease in the TV genome (Farkas et al., 2008). In this study we have demonstrated that both the GST-fusion and his-tagged TV proteases were functionally active using an *in trans* assay on recombinant polyprotein fragments and synthetic substrates. The precise boundaries of the protease were also mapped by the N-terminal sequencing analysis.

In a parallel experiment, we also cloned and expressed the TV protease with upstream sequences including the cleavage site for the TV protease, and demonstrated that the TV protease is capable of auto-cleavage and could release itself from the polyprotein. It is also worthy to note that the expressed TV protease is able to cleave the synthetic peptide containing nine amino acid residues, suggesting that amino acid residues beyond P5 or P5′ may be dispensable for substrate processing by the protease. Successful cleavage of a substrate containing seven amino acid residues by a NoV protease has also been reported (Chang et al., 2012).

The cleavage maps for the nonstructural proteins of several CVs revealed that the substrate cleavage sites of CV proteases are well conserved in this virus family, in which a Glu or Gln is usually present in the P1 position, whereas an Ala or Gly occupies the P1′ position. Based on this conservation of substrate cleavage sites, we proposed a cleavage map for the TV nonstructural polyprotein (Farkas et al., 2008). In this study, four of the five predicted cleavage sites of the TV polyprotein have been experimentally validated using recombinant polyprotein fragments by *in trans* cleavage followed by N-terminal sequencing. The cleavage sites between Vpg and protease, and between protease and RdRp share the same dipeptide residues of E/G. The amino acid residues at the other two sites seemed variable with Q/S between the helicase and 3A-like protein and E/A between 3A-like protein and Vpg. The cleavage at Q/S or E/A sites seems to be more efficient than at the E/G sites, according to the band intensities of the cleaved products (data not shown). Although the cleavage site between N-terminus protein and NTPase could not be validated by the N-terminal sequence analysis, the Q/S scissile bond at amino acid residues 233–234 remains to be the primary candidate for the cleavage, because this was the only one could potentially be cleaved by TV protease within the adjacent 133 amino acid residues. Despite a lack of example for other calicivirus proteases, our result on the cleavage between helicase and 3A-like protein suggested that the Q/S scissile bond could be an efficient cleavage site for CV protease (Fig. 2B).

In addition to the differences in scissile bonds at various cleavage sites, amino acid residues at P2-5 and P2′-5′ also influence the cleavage efficiencies of proteases (Nakamura et al., 2005; Oka et al., 2009). As shown in Table 2, the protease cleavage sites of polyproteins from the CV family are well conserved. It is interesting to note that a Q at the P1 position appears more often in between the N-terminal protein and helicase, and between the helicase and 3A-like protein; whereas an E at the P1 position appears more often between Vpg and the protease and between the protease and RdRp. Vpg, protease, and RdRp have been known to co-exist as precursor protein fragments during the early stage of polyprotein processing (Belliot et al., 2003). The differential preference for specific amino acid residues at the P1 position could be one of the regulatory mechanisms in the control of polyprotein processing.

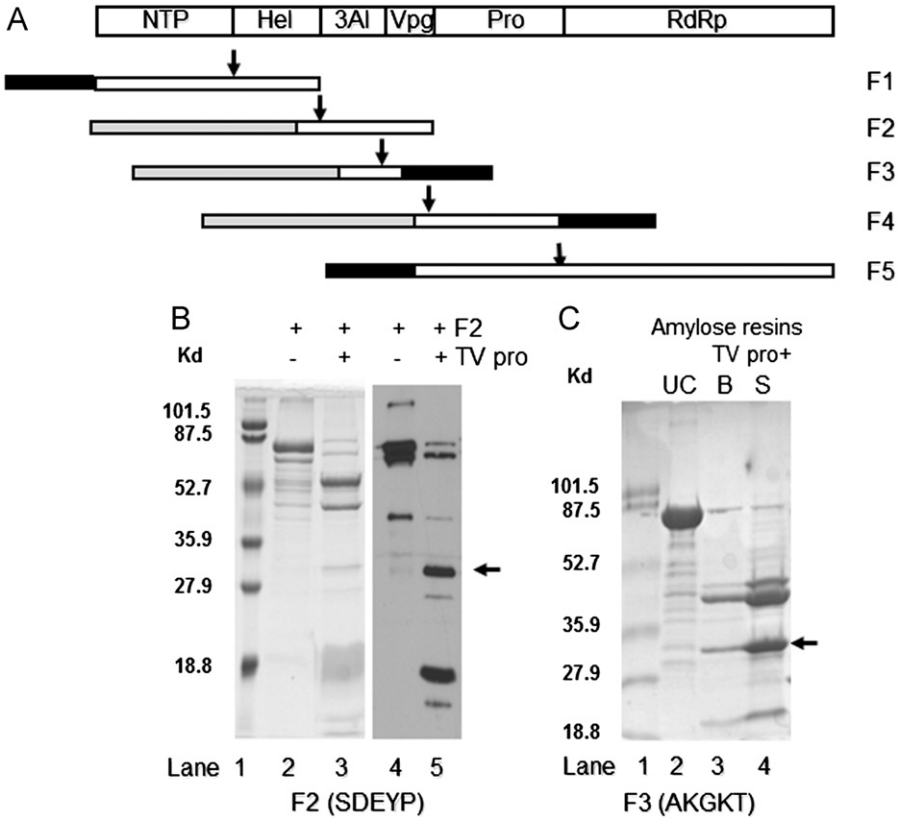

Fig. 2. Expression of TV polyprotein fragments for protease cleavage site mapping. (A) Predicted TV non-structural polyprotein and cloning strategy for mapping analysis. Each fusion protein contains at least one predicted protease cleavage site, as indicated by an arrow. Open boxes represent TV polyprotein fragments; Black boxes represent GST; Grey boxes represent MBP. (B) Cleavage of fragment 2 (helicase-3Alike). Lane 1, protein markers. Lane 2 & 4, undigested fragment 2. Land 3 & 5, digested fragment 2. Lane 4 & 5 were detected with rabbit anti-3A like antibodies. The arrow indicates the protein fragment isolated for N-terminal sequencing analysis. The results of the N-terminal sequencing were shown in the bracket. (C) Cleavage of fragment 3 (3A like-VpG). Lane 1, protein markers. Lane 2, undigested fragment 3. Land 3, digested fragment 3, bound fraction. Lane 4, digested fragment 3, supernatant fraction. The arrow indicates the protein fragment isolated for N-terminal sequencing analysis. The results of the N-terminal sequencing were shown in the bracket.

In this study, we also characterized the enzymatic activities of recombinant TV protease and a NoV protease using FRET substrates. FRET protease assays have been used in characterizations of several viral proteases, such as those of the SARS-Coronavirus (Blanchard et al., 2004; Grum-Tokars et al., 2008), hepatitis C virus (Mao et al., 2008; Santos et al., 2009), yellow fever virus (Kondo et al., 2011), and foot-and-month disease virus (Jaulent et al., 2007). During the preparation of the manuscript, Chang et al. also reported the characterization and inhibition of proteases of two norovirus genogroups using FRET assays (Chang et al., 2012). Unlike other reports on FRET protease activity assays, the Hylite Fluor488 dye and QXL520 quencher were used to label the peptide substrates in our study. Hylite Fluor488 is a new type of fluorophore that provides superior fluorescence quantum yield and a longer emission wavelength, whereas QXL520 has been proven to be an efficient quencher for Hylite Fluor488. The Hylite Fluor 488/QXL520-based FRET peptide shows less interference from autofluorescence of test compounds, thus providing a better assay sensitivity. Our results showed that this newly developed fluorescent dye and quencher pair was effective for the assay. Optimization experiments with the NoV protease showed that the protease was mostly active at a pH between 8 and 8.5, without the need for additional ionic salts. This optimal pH is very similar to that reported for the Chiba virus in NoV genogroup II (Someya et al., 2005). While the presence of glycerol enhanced the protease activities, a low concentration of DMSO (up to 10%) did not affect the enzyme activities. This is important for our future studies in the screening for inhibitors against the NoV protease, because most synthetic compounds are dissolved in DMSO. We also found that the TV and NoV proteases can cleave each other's substrate in the PRET assays. Since NoVs remain uncultivable in vitro, the observed reciprocal enzymatic activities between the NoV/TV proteases suggest that TV could serve as a surrogate for NoVs in future antiviral designs targeting at the protease.

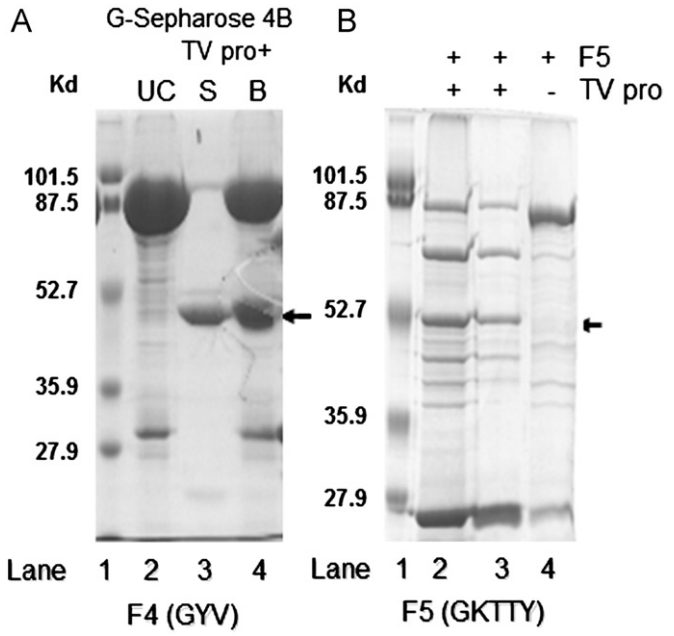

Fig. 3. Mapping of VpG-Pro and Pro-RdRp cleavage sites. (A) Cleavage of fragment 4 (VpG-protease). Lane 1, protein markers. Lane 2, undigested fragment 4. Land 3, digested fragment 4, supernatant fraction. Lane 4, partially digested fragment 4, bound fraction. The arrow indicates the protein fragment isolated for N-terminal sequencing analysis. The results of the N-terminal sequencing were shown in the bracket. (B) Cleavage of fragment 5 (pro-RdRp). Lane 1, protein markers. Lane 2 & 3, digested fragment 5. Land 4, undigested fragment 5. The arrow indicates the protein fragment isolated for N-terminal sequencing analysis. The results of the N-terminal sequencing were shown in the bracket.

In summary, we have four out of the five cleavage sites of the TV polyprotein confirmed by protein N-terminal sequencing analysis. We also established a convenient FRET assay system, which will allow us to screen compound libraries for antivirals

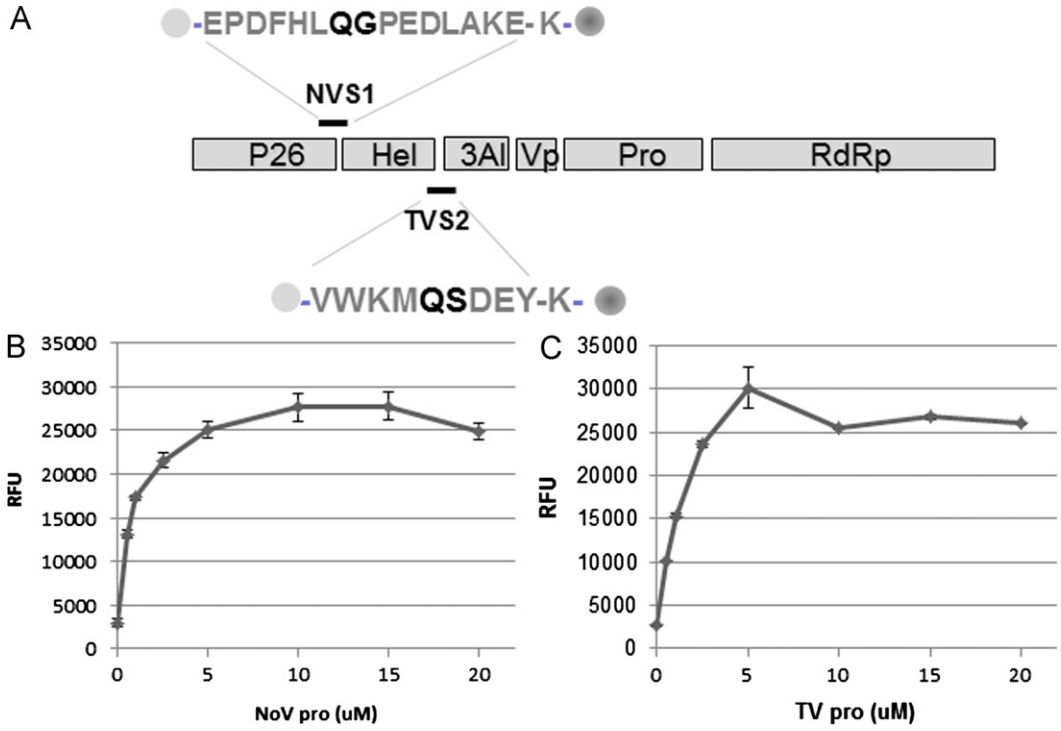

Fig. 4. Determination of enzymatic activities of NoV and TV proteases. (A) Fluorogenic peptide substrates NVS1 (HyliteFlour488-EPDFHLQGPEDLAKE-K (QXL520)–NH2), derived from the cleavage site between N-terminal protein and helicase of NoV polyprotein; and TVS2 (Hylite Flour488-VWKMQSDEY-K(QXL520)–NH2), derived from the cleavage site between helicase and 3A-like of TV polyprotein. (B) Enzymatic activities of NoV protease, and (C) Enzymatic activities of TV protease.

targeting the proteases of NoV/TV. In addition, we have demonstrated specific inhibition of NoV/TV proteases by conventional cysteine protease inhibitors. Furthermore, we have demonstrated the reciprocal substrate cleavage between TV and NoV proteases. Thus, we are in an excellent position to utilize the TV as a model for in vivo screening and evaluation of candidates of protease inhibitors for the uncultivable human NoVs.

Methods

Fluorogenic substrates. Fluorogenic peptide substrates—NVS1 (Hylite Fluor488-EPDFHLQGPEDLAKE-K (QXL520)-NH2) and TVS2 (Hylite Fluor488-VWKMQSDEY-K(QXL520)-NH2) – were designed based on the cleavage site between the N-terminal protein and helicase of the NoV polyprotein (Belliot

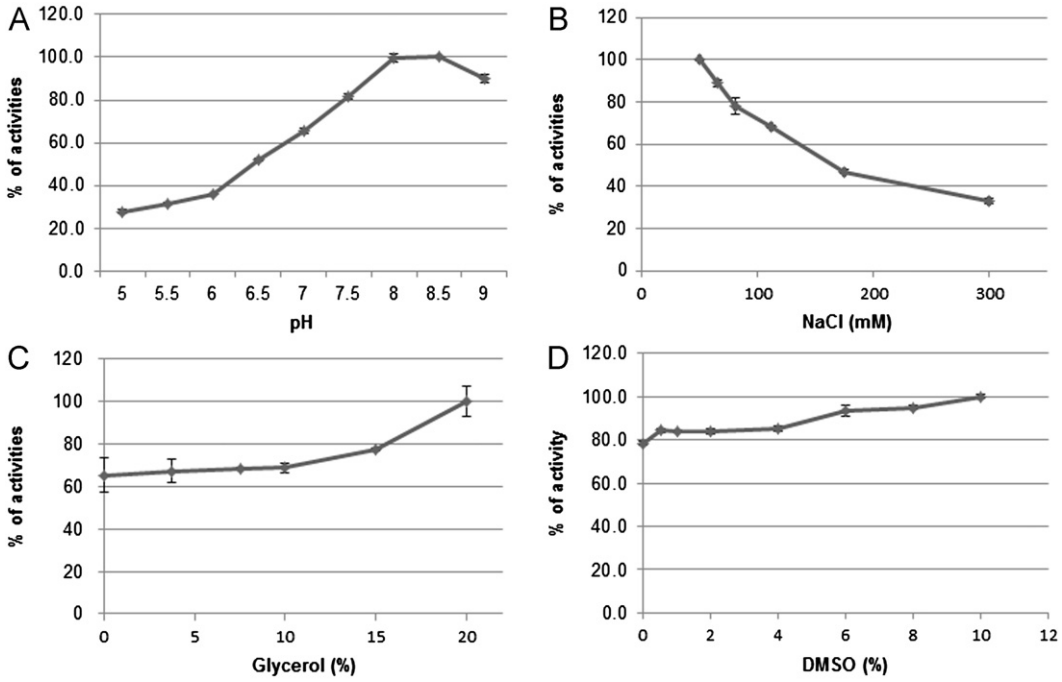

Fig. 5. Effects of pH, NaCl, glycerol, and DMSO on enzymatic activities of NoV protease. (A) Effect of pH. % of protease activity was determined by comparing relative fluorescence units at various reaction conditions to the one with the highest activities (100%). (B) Effect of ionic strength. Same conditions as A at pH 8.5 with varying ionic strength (NaCl: 50 mM, 65.6 mM, 81.3 mM, 112.5 mM, 175 mM, and 300 mM). (C) Effect of glycerol concentration. Same conditions as A at pH 8.5 with addition of glycerol at 0, 3.75, 7.5, 10, 15, and 20%. (D) Effect of DMSO. Same conditions as A at pH 8.5 with addition of DMSO at 0, 0.5, 1, 2, 4, 6, 8, and 10%.

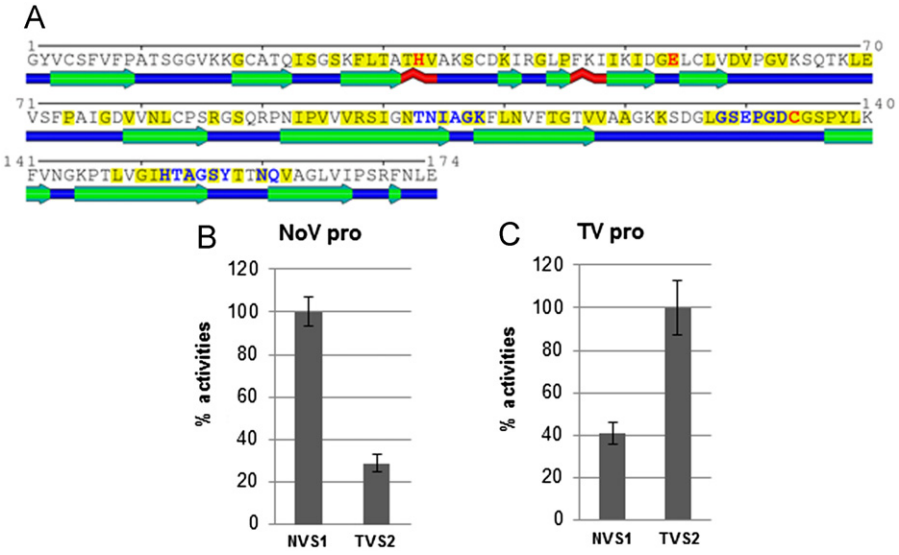

Fig. 6. Predicted secondary structures and active site residues in TV protease, and the reciprocal substrate cleavages of the TV and NoV proteases. (A) Predicted secondary structures and active site residues in TV protease. The predicted beta strands are represented by green arrows, whereas predicted loops and helical turns are shown in blue and red, respectively. Residues conserved or conservatively substituted (while conserving physico-chemical properties) between NoV and TV proteases are highlighted using yellow background. Active site residues are highlighted in red, and residues in contact with a peptide inhibitor in 2IPH (and thus defining the overall substrate binding cleft) are shown in blue. Notice that the active site and substrate binding cleft are within regions conserved between NoV and TV proteases (yellow patches). (B) The relative enzymatic activities of NoV protease on TV protease substrate TVS2, in comparison to on its native substrate NVS1. (C) The relative enzymatic activities of TV protease on NoV protease substrate NVS1, in comparison to on its native substrate TVS2. (For interpretation of the references to color in this figure legend, the reader is refferred to the web version of this article.)

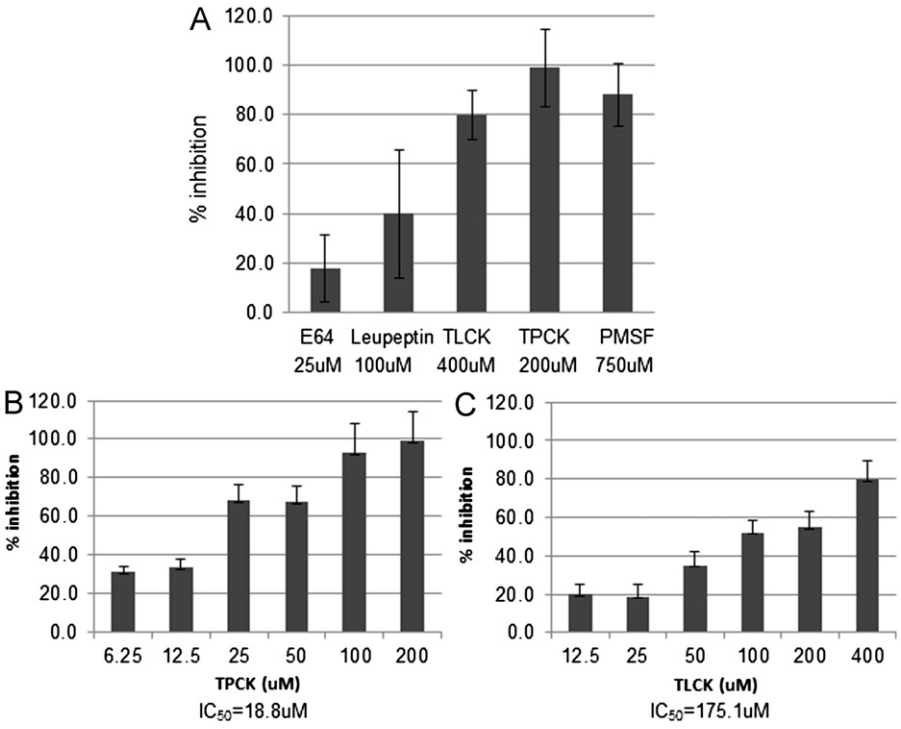

Fig. 7. Inhibition of NoV protease activities by common protease inhibitors. (A) Percent inhibition of NoV protease activities by E64, leupeptin, PMSF, TPCK, and TLCK. (B) IC_{50} of TPCK on NoV protease activities; (C) IC_{50} of TLCK on NoV protease activities.

et al., 2003) or the cleavage site between the helicase and 3A-like protein of the TV polyprotein (Farkas et al., 2008), respectively. Both substrates were synthesized and labeled by Anaspec (CA). The two fluorophores on each substrate form a quenching pair and exhibit FRET within the intact peptide. Upon the cleavage between *Q* and *G* residues on NVS1 by NoV protease, or between *Q* and *S* residues on TVS2 by TV protease (Fig. 4A), the donor fluorophore (Hylite Fluor488) separates from the quenching fluorophore (QXL520), allowing activities of protease to be measured. Stock solution of the fluorogenic substrate was prepared in dimethyl sulfoxide (DMSO), and subsequent dilution was prepared with the assay buffer (50 mM Tris (pH 8.5), 20% glycerol, and 1 mM DTT).

Generation of protease expression constructs. To express the glutathione S-transferase (GST)-protease fusion proteins in *E.coli*, protease coding sequences were amplified from NoV cDNA (Genbank#: NC_001959) with primers p1405B and p1406 (Table 1), and TV cDNA (Genbank#: EU391643) with primers p1069c and p1071b (Table 1), respectively, and were cloned into vector pGEX4T1 (GE Health-care, PA) at BamHI/SalI sites. To express N-terminal histidine (his)-tagged proteases, the same inserts were cloned into vector pQE30 (Qiagen, CA) at the identical cloning sites.

Generation of recombinant TV polyprotein fragment expression constructs. To express TV polyprotein fragments containing predicted protease cleavage sites in the forms of maltose binding protein (MBP) or GST-fusion proteins, the corresponding TV cDNAs (Genbank#: EU391643) were amplified with specific primers (Table 1), and cloned into vector pMAL-c2X (New England Biolab, MA) or vector pGEX4T1 (GE Health-care, PA) (Fig. 2A).

Protein expression and purification. GST-protease fusion proteins, GST-polyprotein fragment fusion proteins, and MBP-polyprotein fragment fusion proteins were expressed in *E.coli* BL21 (DE3) plysS (EMD Millipore, MA) under the induction of 0.4 mM isopropyl β-D-1-thiogalactopyranoside (IPTG) overnight at room temperature. The his-tagged proteases were expressed in *E. coli* M15 (Qiagen, CA) under the identical induction and culture condition. The cells were harvested by centrifugation at $5000 \times g$ for 15 min.

For GST-fusion protein purification, the cell pellets were resuspended in 1X PBS with 1 mM phenylmethylsulfonyl fluoride (PMSF). For MBP-fusion protein purification, the cell pellets were resuspended in column buffer (20 mM Tris–HCl, pH 7.4, 200 mM NaCl, 1 mM EDTA) with 1 mM PMSF. For his-tagged protease purification, the cell pellets were resuspended in cell resuspension buffer (50 mM NaH_2PO_4, pH 8.0, 300 mM NaCl, 10 mM imidazole) with 1 mM PMSF. The cell resuspensions were subjected to sonication, then cell lysates were centrifuged at $12{,}000 \times g$ for 60 min. MBP-, GST-fusion and his-tagged proteins were purified by affinity chromatography using amylose resins (New England Biolabs, MA), Glutathione Sepharose 4B resins (GE Healthcare, PA), or Talon cell trus affinity resins (Clontech, CA).

Purified GST-fusion proteases were further digested with thrombin and subsequently purified with gel permeation chromatography using a Superdex 200 gel filtration column (GE Healthcare, PA). The elution profile was monitored by measuring UV absorbance at 280 nm and the elution fractions were collected and dialyzed with protease buffer (50 mM Tris–HCl, pH7.6, 1 mM EDTA, 50 mM NaCl, 1 mM DTT) (Blakeney et al., 2003), while his-tagged proteases were dialyzed with buffer containing 50 mM NaH_2SO_4, pH4.5, 50 mM NaCl, 10 mM mercaptoethanol (Zeitler et al., 2006). Proteases were then stored at $-80\,^{\circ}C$ in small aliquots. The purity of the proteins was verified with SDS PAGE and protein concentrations were determined using the Bradford protein concentration assay (BioRad, CA).

Protease activity analysis using fluorogenic peptide substrates. For protease activity assays, 2 μM of each protease was mixed with 10 nM of fluorogenic peptide substrate NVS1 or TVS2 in protease buffer, and were transferred to black 96-well non-treated microtiter plates (Corning, NY), with final reaction

Table 2
Summary of verified protese cleavage sites of polyproteins in Calicivirus family.

Virus	N-terminal protein/ NTPase	NTPase/3A-like protein	3A-like protein/Vpg	Vpg/protease	Protease/RdRp	Reference
hNoV (GI- Sothampton)	LQ/GP	LQ/GK	ME/GK	FE/AP	LE/GG	Liu et al. (1999)
hNoV (GII-MD145)	LQ/GP	LQ/GP	TE/GK	FE/AP	LE/GD	Belliot et al. (2003)
MNV	AE/GP	LQ/NK	SE/GK	FE/AP	FQ/GP	Sosnovtsev et al. (2006)
TV	(PQ/SP)	MQ/SD	FE/AK	DE/GY	LE/GK	Farkas et al. (2008) & this paper
FCV	SE/DV	AE/NG	SE/AK	EE/SG	/	Sosnovtsev et al. (2002)
Sapovirus	AQ/GP	EQ/AG	EE/AK	EE/AP	/	Oka et al. (2005, 2009)
RHDV	VE/GV	FE/GA	DQ/GV	YE/GL	ME/GK	Joubert et al. (2000), Wirblich et al. (1995)

volume of 50 μl/well. The reaction mixtures were incubated for 60 min at 37 °C. The fluorescence was detected using Multimode detector 880 (Beckman Coulter, CA) with excitation at 480 nm and emission at 520 nm, respectively. The protease activities were determined from averages of duplicate or triplicate tests.

Optimization of reaction conditions. To determine the effects of pH, ionic strength, glycerol, and dimethyl sulfoxide (DMSO) on the enzymatic activities of the NoV protease, the concentrations of individual buffer components in the standard protease activity assay conditions described above were adjusted. The pH profile was determined at constant ionic strength with a pH range from 5.0 to 9.0, using a variety of buffers suitable for various pHs: 50 mM 2-(N-morpholino) ethanesulfonic acid (MES), 1 mM EDTA, 50 mM NaCl, 1 mM DTT for pH 5–6.5; or 50 mM Tris–HCl, 1 mM EDTA, 50 mM NaCl, 1 mM DTT for pH 7–9 (Nall et al., 2004). The percentage of enzymatic activities was determined by comparing mean relative fluorescent units (RFU) at various points to the highest RFU in the same set of assays.

Polyprotein cleavage and peptide N-terminal sequencing. Purified TV polyprotein fragments and purified TV protease were incubated at room temperature overnight. The cleaved products were run on SDS gels and blotted to PVDF membranes. After staining with Coomassie brilliant blue R-250, the desired bands were excised for the peptide N-terminal sequencing. The peptide N-terminal sequencing services were performed by the protein facility at Iowa State University, Ames, IA.

Prediction of the secondary structures and active site residues in TV protease. BLASTp was used to align TV protease sequence to the closest structurally resolved NoV protease (PDB code 2IPH), which allowed us to map secondary structures from the NoV template into TV protease between residues 18 and 162. For the remaining N- and C-termini residues, secondary structures predicted by SABLE (http://sable.cchmc.org) are used to provide the overall predicted structure of TV protease.

Inhibition assays. To allow formation of enzyme/inhibitor complexes, 2 μM of each protease was pre-incubated with inhibitors at desirable concentrations in protease buffer at room temperature for 30 min. The proteolytic reaction was then initiated by the addition of the fluorogenic peptide substrates (2.5 μM). The final reaction mixtures were transferred to black, 96-well non-treated microtiter plates and were incubated for 60 min at 37 °C. The fluorescence emissions were measured in triplicate for each data point, as described above. Percent inhibition was determined by comparing the mean RFU of each reaction with inhibitors to the corresponding mean RFU of the reaction without inhibitors. The IC_{50} values were determined from reaction mixtures containing various concentrations of inhibitors ranging from 0 to 1000 μM.

Generation of mouse anti-TV-3Al antibodies. The coding region of TV 3Al (aa574-712) was amplified with primers p1282b and p1283b (Table 1), and was cloned into pQE30 vector (Qiagen). The his-TV3Al protein was then expressed in *E.coli* M15 (Qiagen) under the induction of 0.4 mM isopropyl β-D-1-thiogalactopyranoside (IPTG) for overnight at room temperature. The cells were harvested by centrifugation at 5000 × *g* for 15 min. To purify the his-3Al protein, the cell pellets were resuspended 1*x* lysis buffer (50 mM NaH_2PO_4, pH8.0, 300 mM NaCl, and 10 mM imidazole) containing 1 mM phenylmethylsulfonyl fluoride (PMSF). The cell resuspensions were then subjected to sonication, and the cell lysates were then centrifuged at 12,000 × *g* for 60 min. The recombinant protein was purified by affinity chromatography using TALON His-Tag Purification Resin (Clonetech). Mouse anti-TV3Al polycolonal antibodies were generated follow a conventional antibody generation procedure.

Acknowledgement

We thank Christina Quigley for critical reviews of the manuscript. This study was supported by the National Institutes of Health (R01 AI37093, R01 AI55649 and P01 HD013021) and Department of Defense (PR033018) to X.J.

References

Belliot, G., Sosnovtsev, S.V., Mitra, T., Hammer, C., Garfield, M., Green, K.Y., 2003. In Vitro proteolytic processing of the MD145 norovirus ORF1 nonstructural polyprotein yields stable precursors and products similar to those detected in calicivirus-infected cells. J. Virol. 77, 10957–10974.

Blakeney, S.J., Cahill, A., Reilly, P.A., 2003. Processing of Norwalk virus nonstructural proteins by a 3C-like cysteine proteinase. Virology 308, 216–224.

Blanchard, J.E., Elowe, N.H., Huitema, C., Fortin, P.D., Cechetto, J.D., Eltis, L.D., Brown, E.D., 2004. High-throughput screening identifies inhibitors of the SARS coronavirus main proteinase. Chem. Biol. 11, 1445–1453.

Chang, K.O., Takahashi, D., Prakash, O., Kim, Y., 2012. Characterization and inhibition of norovirus proteases of genogroups I and II using a fluorescence resonance energy transfer assay. Virology 423, 125–133.

Farkas, T., Sestak, K., Wei, C., Jiang, X., 2008. Characterization of a rhesus monkey calicivirus representing a new genus of Caliciviridae. J. Virol 82, 5408–5416.

Glass, P.J., White, L.J., Ball, J.M., Leparc-Goffart, I., Hardy, M.E., Estes, M.K., 2000. Norwalk virus open reading frame 3 encodes a minor structural protein. J. Virol 74, 6581–6591.

Glass, R.I., Parashar, U.D., Estes, M.K., 2009. Norovirus gastroenteritis. N. Engl. J. Med. 361, 1776–1785.

Grum-Tokars, V., Ratia, K., Begaye, A., Baker, S.C., Mesecar, A.D., 2008. Evaluating the 3C-like protease activity of SARS-Coronavirus: recommendations for standardized assays for drug discovery. Virus Res. 133, 63–73.

Hussey, R.J., Coates, L., Gill, R.S., Wright, J.N., Sarwar, M., Coker, S., Erskine, P.T., Cooper, J.B., Wood, S., Clarke, I.N., Lambden, P.R., Broadbridge, R., Shoolingin-Jordan, P.M., 2010. Crystallization and preliminary X-ray diffraction analysis of the protease from Southampton norovirus complexed with a Michael acceptor inhibitor. Acta Crystallogr. Sect. F Struct. Biol. Cryst. Commun. 66, 1544–1548.

Jaulent, A.M., Fahy, A.S., Knox, S.R., Birtley, J.R., Roque-Rosell, N., Curry, S., Leatherbarrow, R.J., 2007. A continuous assay for foot-and-mouth disease virus 3C protease activity. Anal. Biochem. 368, 130–137.

Jiang, X., Wang, M., Wang, K., Estes, M.K., 1993. Sequence and genomic organization of Norwalk virus. Virology 195, 51–61.

Joubert, P., Pautigny, C., Madelaine, M.F., Rasschaert, D., 2000. Identification of a new cleavage site of the 3C-like protease of rabbit haemorrhagic disease virus. J. Gen. Virol. 81, 481–488.

Kondo, M.Y., Oliveira, L.C., Okamoto, D.N., de Araujo, M.R., Duarte dos Santos, C.N., Juliano, M.A., Juliano, L., Gouvea, I.E., 2011. Yellow fever virus NS2B/NS3 protease: hydrolytic properties and substrate specificity. Biochem. Biophys. Res. Commun. 407, 640–644.

Leung, D., Schroder, K., White, H., Fang, N.X., Stoermer, M.J., Abbenante, G., Martin, J.L., Young, P.R., Fairlie, D.P., 2001. Activity of recombinant dengue 2 virus NS3 protease in the presence of a truncated NS2B co-factor, small peptide substrates, and inhibitors. J. Biol. Chem. 276, 45762–45771.

Liu, B.L., Viljoen, G.J., Clarke, I.N., Lambden, P.R., 1999. Identification of further proteolytic cleavage sites in the Southampton calicivirus polyprotein by expression of the viral protease in *E. coli*. J. Gen. Virol. 80, 291–296, Pt 2.

Mao, S.S., DiMuzio, J., McHale, C., Burlein, C., Olsen, D., Carroll, S.S., 2008. A time-resolved, internally quenched fluorescence assay to characterize inhibition of hepatitis *C* virus nonstructural protein 3-4A protease at low enzyme concentrations. Anal. Biochem. 373, 1–8.

Nakamura, K., Someya, Y., Kumasaka, T., Ueno, G., Yamamoto, M., Sato, T., Takeda, N., Miyamura, T., Tanaka, N., 2005. A norovirus protease structure provides insights into active and substrate binding site integrity. J. Virol. 79, 13685–13693.

Nall, T.A., Chappell, K.J., Stoermer, M.J., Fang, N.X., Tyndall, J.D., Young, P.R., Fairlie, D.P., 2004. Enzymatic characterization and homology model of a catalytically active recombinant West Nile virus NS3 protease. J. Biol. Chem. 279, 48535–48542.

Oka, T., Katayama, K., Ogawa, S., Hansman, G.S., Kageyama, T., Ushijima, H., Miyamura, T., Takeda, N., 2005. Proteolytic processing of sapovirus ORF1 polyprotein. J. Virol. 79, 7283–7290.

Oka, T., Yokoyama, M., Katayama, K., Tsunemitsu, H., Yamamoto, M., Miyashita, K., Ogawa, S., Motomura, K., Mori, H., Nakamura, H., Wakita, T., Takeda, N., Sato, H., 2009. Structural and biological constraints on diversity of regions immediately upstream of cleavage sites in calicivirus precursor proteins. Virology.

Robel, I., Gebhardt, J., Mesters, J.R., Gorbalenya, A., Coutard, B., Canard, B., Hilgenfeld, R., Rohayem, J., 2008. Functional characterization of the cleavage specificity of the sapovirus chymotrypsin-like protease. J. Virol. 82, 8085–8093.

Santos, J.A., Gouvea, I.E., Judice, W.A., Izidoro, M.A., Alves, F.M., Melo, R.L., Juliano, M.A., Skern, T., Juliano, L., 2009. Hydrolytic properties and substrate specificity of the foot-and-mouth disease leader protease. Biochemistry 48, 7948–7958.

Someya, Y., Takeda, N., 2009. Insights into the enzyme-substrate interaction in the norovirus 3C-like protease. J. Biochem. 146, 509–521.

Someya, Y., Takeda, N., Miyamura, T., 2005. Characterization of the norovirus 3C-like protease. Virus Res. 110, 91–97.

Sosnovtsev, S.V., Belliot, G., Chang, K.-O., Prikhodko, V.G., Thackray, L.B., Wobus, C.E., Karst, S.M., Virgin, H.W., Green, K.Y., 2006. Cleavage map and proteolytic processing of the murine norovirus nonstructural polyprotein in infected cells. J. Virol. 80, 7816–7831.

Sosnovtsev, S.V., Garfield, M., Green, K.Y., 2002. Processing map and essential cleavage sites of the nonstructural polyprotein encoded by ORF1 of the feline calicivirus genome. J. Virol. 76, 7060–7072.

Wei, C., Farkas, T., Sestak, K., Jiang, X., 2008. Recovery of infectious virus by transfection of in vitro-generated RNA from Tulane calicivirus cDNA. J. Virol. 82, 11429–11436.

Wirblich, C., Sibilia, M., Boniotti, M.B., Rossi, C., Thiel, H.J., Meyers, G., 1995. 3C-like protease of rabbit hemorrhagic disease virus: identification of cleavage sites in the ORF1 polyprotein and analysis of cleavage specificity. J. Virol. 69, 7159–7168.

Zeitler, C.E., Estes, M.K., Venkataram Prasad, B.V., 2006. X-ray crystallographic structure of the Norwalk virus protease at 1.5—A resolution. J. Virol. 80, 5050–5058.